Article type: Original research article

Title: Magnetisation transfer ratio measures in normal appearing white matter show periventricular gradient abnormalities in multiple sclerosis

Authors: Zheng Liu (1, 2)*, Matteo Pardini (1, 3)*, Özgür Yaldizli (1, 4), Varun Sethi (1), Nils Muhlert (1, 5), Claudia AM Wheeler-Kingshott (1), Rebecca S Samson (1), David H Miller (1, 6) and Declan T Chard (1, 6)

* These authors contributed equally to this work.

Affiliations

1: Queen Square MS Centre, NMR Research Unit, Department of Neuroinflammation, UCL Institute of Neurology, London, UK

2. Department of Neurology, Xuanwu Hospital of Capital Medical University, Beijing 100053, China

3. Department of Neuroscience, Rehabilitation, Ophthalmology, Genetics, Maternal and Child Health, University of Genoa, Genoa, Italy.

4. MS Centre, Department of Neurology, University Hospital Basel, Basel, Switzerland

5. School of Psychology and Cardiff University Brain Research Imaging Centre, Cardiff University, Cardiff, UK

6. National Institute for Health Research (NIHR) University College London Hospitals (UCLH) Biomedical Research Centre, UK

Corresponding author: Declan Chard

Address: Queen Square Multiple Sclerosis Centre, Department of Neuroinflammation, UCL Institute of Neurology, University College London, Queen Square, London, WC1N 3BG, UK.

Telephone number: +44 2078298771

Email: d.chard@ucl.ac.uk

Running title: Periventricular MTR gradients in MS

Abstract: 394 words

Main document: 3524 words

Tables: 3

Figures: 4

References: 38

Abstract

In multiple sclerosis (MS), there is increasing evidence that demyelination, and neuronal damage within and beyond lesions, occurs preferentially in cortical grey matter (GM) next to the outer surface of the brain. It has been suggested that this may be due to the effects of pathology outside the brain parenchyma, in particular meningeal inflammation or through cerebrospinal fluid (CSF) mediated factors. White matter (WM) lesions are often located adjacent to the ventricles of the brain, suggesting the possibility of a similar outside-in pathogenesis, but an investigation of the relationship of periventricular normal-appearing (NA) WM abnormalities with distance from the ventricles has not previously been undertaken. The present study investigates this relationship *in vivo* using quantitative MR imaging and compares the abnormalities between SPMS and relapsing remitting (RR) MS. Forty-three people with RRMS and 28 with SPMS, and 38 healthy controls, were included in this study. T1-weighted volumetric, magnetisation transfer (MT) and PD/T2-weighted scans were acquired for all subjects. From the MT data, MT ratio (MTR) maps were prepared. WM tissue masks were derived from SPM8 segmentations of the T1-weighted images. NAWM masks were generated by subtracting WM lesions identified on the PD/T2 scan, and a 2 voxel perilesional ring, from the SPM8 derived WM masks. WM was divided in concentric bands, each about 1 mm thick, radiating from the ventricles toward the cortex. The first periventricular band was excluded from analysis to mitigate partial volume effects, and NAWM and lesion MTR values were then

computed for the ten bands nearest to the ventricles. Compared with controls, MTR in the NAWM bands was significantly lower in MS. In controls, MTR was highest in the band adjacent to the ventricles and declined with increasing distance from the ventricles. In the MS groups, relative to controls, reductions in MTR were greater in the SPMS compared with RRMS group, and these reductions were greatest next to the ventricles and became smaller with distance from them. WM lesion MTR reductions were also more apparent adjacent to the ventricle and decreased with distance from the ventricles in both the RR and SPMS groups. These findings suggest that in people with MS, and more so in SPMS than RRMS, tissue structural abnormalities in NAWM and WM lesions are greatest near the ventricles. This would be consistent with a CSF or ependymal mediated pathogenesis.

Key words: multiple sclerosis, magnetisation transfer ratio, normal appearing white matter,

Introduction

The pathogenesis of progressive multiple sclerosis (MS) remains unknown, but recent studies have raised the possibility of factors external to the brain parenchyma playing a significant role. In people with secondary progressive (SP) MS, grey matter (GM) lesions may be as or more extensive than white matter (WM) lesions (Lassmann, 2013; Bo et al., 2003), and GM lesions are much more abundant in the outer (subpial) cortical layers when compared with the cortex next to WM (Bo et al., 2003). Similarly, neuronal loss in MS may be substantial in the cortex (Wegner et al., 2006), and is also greatest in the outer (subpial) compared with inner cortical layers (Magliozzi et al., 2010). This gradient in cortical GM lesions and neuronal pathology has been linked with meningeal inflammation, in particular the presence of B-cell follicle-like aggregates in secondary progressive (SP) MS (Magliozzi et al., 2010; Magliozzi et al., 2007), and it has been suggested that meningeal inflammation or CSF-mediated factors may play a key pathogenic role in cortical pathology.

WM lesions occur more frequently around the ventricle than elsewhere, and a clear explanation for this distribution has not been found (Narayanan et al., 1997). They appear to form around veins, and in the case of periventricular lesions around subependymal veins (Adams et al., 1987), but the mechanism for this has not been determined. Perivascular (venous) inflammatory infiltrates are seen in MS lesions (Adams, 1975), but it is not known if they are

necessary for lesion genesis or part of a more chronic process. Tissue hypoxia has been suggested as having a pathogenic role in lesion formation (Lassmann, 2003), and for haemodynamic reasons periventricular WM may be more likely than other parts of the brain to become hypoxic, explaining the predilection for lesion formation in this region (Beggs, 2013). Patchy “granular ependymitis” has also been observed in a single study by Adams et al. (Adams et al., 1987), although only co-localised with about 1 in 10 periventricular lesions.

In light of findings in cortical GM, which suggest a possible outside-in pathogenesis, it would be of interest to know if the characteristics of normal-appearing (NA) WM were also dependent on their location relative to the ventricular CSF interface. However, there is a paucity of histopathological or magnetic resonance imaging (MRI) studies that have looked for such an association in periventricular NAWM. One histopathological study looked at WM lesion features dependent on their distance from the ventricles, specifically looking at glial progenitor cell density, and found that it was highest in the lesions in the sub ventricular (sub ependymal) zone (Nait-Ousmesmar et al. 2007). One MRI study looked at WM lesion features dependent on their distance from the ventricles, which found that lesions are more likely to be hypo-intense on T1-weighted images the closer they are to the ventricles (Papadopoulou et al., 2014).

Magnetisation transfer ratio (MTR) is a magnetic resonance imaging (MRI) technique that has proven sensitive to MS pathology in WM lesions and

NAWM (Horsfield, 2005). In combined MRI and histopathological studies, reductions in MTR have been found to correlate with both demyelination and axonal loss, and as such it is sensitive to two major elements of WM pathology in MS (Schmierer et al., 2004). With recent technical advances, it is now possible to obtain MTR maps at 1mm isotropic resolutions, and this has allowed us to subdivide the cortex into inner and outer bands. We found a preferential MS disease effect on the outer (subpial) relative to the inner cortex in people with SPMS (Samson et al., 2014).

In this work, using the same high resolution MTR method, we aimed to investigate two questions:

1. In people with RRMS and SPMS, is there a relationship between NAWM and WM lesion MTR, and distance from the ventricles?
2. Are periventricular NAWM and lesion MTR abnormalities more prominent in SPMS compared with RRMS?

Materials and Methods

Subjects

Participants were between 18 and 65 years old. Those with MS had to have a diagnosis of clinically definitive MS according to McDonald criteria (Polman et al. 2005), and MS subtypes were classified using the Lublin-Reingold (Lublin et al. 1996) criteria. The control group had to have no known neurological

disease. All participants provided written informed consent. This study was approved by our local institutional ethics committee.

We included 71 people with MS: 43 with RRMS and 28 with SPMS. The mean ± standard deviation (SD) ages were 42.5 ± 10.0and 53.0 ± 8.1 respectively, and disease duration from first symptom onset was 11.7 ± 8.1and 21.9 ± 10.4. Forty-eight (68%) were female. The median EDSS (Kurtzke, 1983) was 5.5 (range 1-8.5). Thirty-five (49%) of the MS group were receiving a disease-modifying treatment at time of the study. Thirty-eight people served as controls, mean (SD) age 39.1 ± 11.9, 21 (55%) females.

Magnetic resonance imaging

Using a 3T Philips Achieva system (Philips Healthcare, Best, The Netherlands) with a 32-channel head coil and multi-transmit technology, the following sequences were acquired: 3D sagittal T1-weighted fast field echo (FFE) scan: 1x1x1 mm^3, inversion time (TI)=824 ms, repetition time (TR)=6.9 ms, echo time (TE)=3.1 ms; dual-echo proton density/T2-weighted axial-oblique scans aligned with the anterior to posterior commissure line (1x1x3 mm^3, TR=3500 ms, TE=19/85 ms); and high resolution MT imaging using a 3D slab-selective FFE sequence with two echoes (1x1x1 mm^3, TR=6.4 ms, TE=2.7/4.3 ms, alpha=9° with and without sinc-Gaussian shaped MT pulses of nominal alpha=360°, offset frequency 1kHz, duration 16ms. A turbo field echo (TFE) readout was used, with an echo train length of four, TFE shot

interval 32.5 ms, giving a total time between successive MT pulses of 50ms, and scan time ~25 minutes). The two echoes were averaged (thereby increasing the SNR) for both the MT on and MT off data used to calculate the MTR.

Image analysis

Segmentation of T1-w 3D images

The T1-weighted scans were segmented using Statistical Parametric Mapping (SPM8; Wellcome Trust Centre for Neuroimaging, London, UK [www.fil.ion.ucl.ac.uk/]; using the new segment pipeline) after WM lesion filling (Chard et al. 2010), and the resultant GM, WM and CSF probability maps were then binarised. To minimise the potential for partial volume effects between tissues, the probability of each voxel being of a given tissue type had to be ≥90% (Samson et al., 2014). In addition, brain parenchymal fraction (BPF; GM and WM tissue volume divided by GM, WM plus CSF volume) was measured using the same SPM8 tissue segmentations, for use as a covariate in the statistical models.

Extraction of normal appearing white matter

WM lesions were identified and contoured on PD/T2 scans using JIM (Version 6.0, Xinapse Systems, Northants). For each participant the WM lesion masks from the PD/T2 images were then co-registered to the corresponding T1-w 3D

scan. To achieve this a pseudo-T1 image was generated by subtracting the PD from the T2-weighted image (Hickman et al., 2002), so providing an image with a similar contrast to the T1-w 3D scan. Using NiftyReg (Modat et al., 2010; Ourselin et al., 2001), a linear transformation was then computed to co-register the pseudo-T1 image to the T1-w 3D image, and then the same transformation was applied to the PD/T2 lesion mask. A previous study has shown that MTR is significantly more abnormal in the WM 1-2mm adjacent to the edge of an MS lesion, as seen on a PD/T2-weighted scan, when compared with WM more distant from the lesion margin (Vrenken et al., 2006). To prevent this from affecting normal appearing (NA) WM MTR measurements in this study, a perilesional tissue mask was prepared by dilating the PD/T2 lesion mask 2 mm in each direction. Binarised WM lesions and perilesional tissue masks were then subtracted from each subject's binarised WM mask to create a NAWM mask. As further precaution against lesion contamination of NAWM, the same analysis was rerun using a 3 voxels dilation of WM lesion masks. The results of this analysis are reported in the Supplementary Materials.

Coregistration of MT data to T1-w images

MT_{on} and MT_{off} images for each subject were affine registered to T1-w volume image using NiftyReg, and MTR maps calculated (MTR = (MT_{off} - MT_{on}) / MT_{off}), measured in percentage units (pu).

Segmentation of WM into concentric periventricular 1 voxel thick bands

For each subject NAWM was segmented into concentric 1 voxel-thick bands starting at the ventricular margin and extending in to the brain parenchyma (Figure 1). To prevent NAWM bands arising simultaneously from the body and temporal horns of the lateral ventricles from clashing, only WM and ventricular CSF superior to the insula were included in the analysis (Figure 1).

For each subject, a mask of the body of the lateral ventricles was first created by linearly co-registering their thresholded CSF map with the lateral ventricle mask included in the Wake Forest University School of Medicine PickAtlas toolbox (Maldjian et al., 2003). This mask was reviewed and if required manually edited (by ZL) to ensure a robust match with lateral ventricle anatomy in each subject. The CSF mask was then repeatedly dilated by 1 voxel (1 x 1 x $1mm^3$) using DilM (part of the FSL software package (http://www.fmrib.ox.ac.uk/fsl/) through NAWM to generate concentric 1 voxel-thick NAWM bands. In each subject, sequential bands were extracted until the volume of any given band fell below 0.5 ml. This yielded a series of NAWM bands extending from the ventricles through to the cortex. As an extra precaution against periventricular CSF-WM partial volume effects, data from the first band was not included in subsequent analyses. As the aim of this study was to look for periventricular MS disease effects, MTR values were extracted for the first 10 NAWM bands (i.e. covering ~1cm of distance between the ventricles and cortex).

WM lesion measures

To calculate WM lesion volumes and MTR values dependent on their distance from the ventricles, a similar procedure to that used to obtain NAWM data was used. Ventricular CSF was sequentially dilated by 1 voxel (as above) through the WM lesion mask, so generating a set of concentric WM lesion masks. Mean and SD WM lesion MTR and volumes were then calculated.

Statistical analyses

Demographic data and MTR values are presented as mean ± SD. EDSS values are presented as median (range). Statistical analyses were computed using SPSS (version 22, IBM). In each subject, MTR values within each NAWM band were averaged. The average MTR in each NAWM band was then separately compared between groups using general linear models, including age and gender as potentially confounding factors. Rather than run different models for each possible pairwise combination of groups, all three study groups (HC, RRMS and SPMS) were included in a single model for each NAWM band, so allowing group differences to be tested simultaneously. As a further precaution against CSF partial volume effects, and to allow for potential differences in the relative alignment of NAWM bands due to disease associated atrophy, both the total number of NAWM bands extracted and BPF were included as additional covariates. Gradients in NAWM MTR were calculated between pairs of bands and divided by the number of intervals spanned (e.g. the MTR gradient between bands 1 and 5 was calculated by

subtracting the mean MTR value in band 5 from that in band 1, and dividing by 4). $P \leq 0.05$ was considered to be the threshold for statistical significance.

Results

Participant demographics, clinical characteristics, and MTR values are given in Table 1. Figure 2 shows the mean (standard error) NAWM MTR in each group. Figure 3a shows the corresponding WM lesion MTR values and Figure 3b the WM lesion volumes.

From Figure 2 it can be seen that in healthy controls, the NAWM MTR was highest in the immediate periventricular NAWM band, and then declined with distance from the ventricles. In people with MS, NAWM MTR was lower than that in controls (Table 2). The MS-associated reduction in MTR was greatest in the NAWM adjacent to the ventricles, and noticeably declined with increasing distance from the ventricles until band 5. Whereas in controls MTR was higher in band 1 than band 5, in MS MTR was higher in band 5 than band 1. We therefore tested between group differences in NAWM MTR in bands 1, 5 and (for reference) 10, and MTR gradients between bands 1 and 5, and 5 and 10.

Compared with controls MTR was significantly lower in bands 1, 5 and 10 in overall MS groups, as well as in RRMS and SPMS subgroups (Table 2). In band 1 MTR was significantly lower in the SPMS compared with RRMS group (Table 2). Age effects were not significant. Gender had a significant effect in

band 5 and 10, however this did not materially alter the observed inter-group differences and so unadjusted results are presented (Table 2). Covarying for BPF or for the number of bands extracted did not materially alter the results, except for the comparison of MTR in band 1 between RRMS and SPMS groups, which reduced the statistical significance of differences between them to a borderline level (see supplemental Table 1). Compared with controls, MTR gradients between bands 1 and 5 differed significantly with both the MS subgroups or overall MS groups (Table 3). Between bands 5 and 10, changes in MTR differed significantly between the control and the MS groups (Table 3). Comparing the MS subgroups, NAWM MTR gradients between bands 1 and 5 were significantly greater in the SPMS compared with RRMS group. Age and gender were not significant in these models, and covarying for the total number of bands or BPF did not materially affect them (see supplemental Table 2), and so unadjusted results are presented.

Lesion MTR and volume by distance from the ventricles is shown in Figure 3 and 4. It can be seen that with distance from the ventricles lesion volume decreases, and from bands 1 to 5 lesion MTR increases. Beyond band 5, lesions volumes are very small, and lesion MTR measures becomes more variable, but as with NAWM, they appear to plateau and then decline, so mirroring (at a lower level) the MTR gradient between bands seen in control WM. Dilating the WM lesion masks by 3 voxels did not materially alter the (see Supplemental Table 3-4 and Supplemental Figure 1).

Discussion

In the MS groups MTR was reduced throughout the NAWM, however the distribution of MTR values did not simply mirror, at a lower level, those in healthy controls. Instead, there was a clearly greater MS disease effect close to the ventricles. Similar findings were noted in WM lesions, with the magnitude of MTR reductions within lesion decreasing with distance from the ventricles. These findings strongly indicate that not only are lesions more likely to occur around the ventricles (Narayanan et al., 1997) (Figure 3b), but pathological changes within NAWM and WM lesions are also greater around the ventricles (Figure 2 and 3a). This suggests that pathology in WM occurs preferentially at or near the inner surface of the brain.

Considering technical factors that may have influenced these results, inclusion of ventricular CSF in the NAWM and WM lesions masks could spuriously reduce periventricular MTR. However, we think this is highly unlikely for four reasons. First, we used a stringent threshold (90%) to binarise the SPM8 tissue segmentations. Second, we discarded MTR data in the first NAWM and WM lesion bands in each subject. Third, covarying for the total number of NAWM bands or BPF (a measure of brain atrophy) in the statistical analyses did not materially alter the results. Fourth, there was no periventicular reduction in MTR seen in controls, and we would expect to see at least a hint of this if partial volume with CSF was significantly affecting periventricular NAWM MTR measures.

It is also highly unlikely that there was any lesion contamination of NAWM (which would reduce NAWM MTR). First, based on work by Vrenken et al. (Vrenken et al., 2006), who demonstrated that perilesional reductions in MTR were detectable for 1 to 2 mm, we dilated our lesion masks by 2 voxels i.e. the linear equivalent of at least 2 mm, making it very unlikely that any residual lesions or perilesional tissues could have contributed significantly to NAWM measures. We also re-ran the analysis dilating lesions by 3 voxels, and this did not materially alter the results (see Supplementary Materials). Secondly, the pattern of changes between bands in NAWM MTR (Figure 2) and WM lesion MTR (Figure 3a) are similar, and this would be difficult to account for through consistent partial volume between them. Further investigation of whether or not periventricular NAWM MTR abnormalities occur independently of lesions could be undertaken by studying subjects who do not have periventricular lesions. We could not investigate this in our cohort as almost all had periventricular lesions, which is usually the case in established MS. A future study of people with clinically isolated syndromes or clinically very early MS – more of whom may not have periventricular lesions – would be of interest.

Brain atrophy could lead to the relative position of NAWM bands differing between people, e.g. band 10 in one person may fall a quarter of the way from the ventricular margin to the cortex, while in another person it may be halfway between them. However, misalignment of NAWM bands due atrophy could not account for the MTR gradients seen (as it will tend to flatten gradients within each group) or differences between groups (as it will increase

variability in group-wide MTR measures within each band). However, as a further precaution we also included both the total number of NAWM bands extracted and BPF as covariates in the statistical models, and this did not materially alter the results.

A gradient in disease-associated MTR reductions was seen in all MS groups, but the periventricular reduction was significantly greater in the SPMS group when compared with RRMS. Several possible mechanisms might contribute to preferential periventricular abnormalities in MS, although with the currently limited information available it is not possible to determine which is the primary one. First, CSF mediated factors may be relevant. This could provide a unifying explanation for the predilection for cortical GM pathology to occur next to the outer surface of the brain (Bo et al., 2003; Magliozzi et al., 2007; Magliozzi et al., 2010; Samson et al., 2014) and the periventricular NAWM MTR gradients seen in the present study. CSF from people with MS has been shown to induce both oligodendrocyte (Hughes and Field, 1967) and neuronal damage in cell cultures (Vidaurre et al., 2014). Secondly, inflammatory activity in the ependyma may be a factor. In a single histopathological study, Adams et al. (1987) found the ependyma overlying periventricular WM to be focally abnormal, and interpreted this as representing ependymitis. Thirdly, it has been suggested that periventricular WM is more likely than other WM regions to become hypoxic when oxygen availability is reduced (Beggs, 2013), although hypoxia is also only thought to be a significant factor in the pathogenesis of a minority of WM lesions (Lucchinetti et al., 2000; Lassmann, 2003).

The differences in the observed MTR gradients between people with MS and healthy controls are very difficult to explain on the basis of technical factors, such as partial volume, alone. However, there are some other limitations to consider. Because of the morphological complexity of dilating the whole ventricular system through WM, and the potential for bands arising from the body of lateral ventricles overlapping with those from the temporal horns, we restricted our analysis to tissues above the insula. In addition, specific pathological interpretation of WM MTR is difficult as it is sensitive to both demyelination and axonal loss (Schmierer et al., 2004), demyelination and axonal loss are highly correlated (Schmierer et al., 2004), and so we cannot determine which is mostly responsible for the gradient seen. In a recent spinal cord study in people with MS, a reduction in MTR has also been observed in the outermost cord voxel layer and, in addition to demyelination and axonal loss, the possibility of a direct effect of inflammatory infiltrates was also raised (Kearney et al., 2014). Quantitative histopathological assessment of the ependyma and periventricular WM is warranted to provide further insight into the cause of the MTR abnormalities observed in this study.

In conclusion, we have found a gradient in MTR abnormalities from periventricular through to deep NAWM in people with MS, with the most marked abnormality seen in the immediate periventricular region and in SPMS. In combination with previous observations about cortical pathology, this suggests that there is a predilection for pathology to occur near the

surface of the brain, particularly in SPMS. The present results highlight the need for further work clarifying the potential role of factors such as CSF mediators, ependymal inflammation, and periventricular tissue hypoxia, in the pathogenesis of lesional and non-lesional abnormalities in MS, and of SPMS.

Acknowledgments

We thank all the people who participated in this study and Daniel Altmann for statistical support.

Funding

ZL was supported by an ECTRIMS (European Committee for Treatment and Research in Multiple Sclerosis) clinical training fellowship. MP thanks the non-profit AKWO association, Lavagna (GE, Italy), for their unrestricted financial support. The NMR Research Unit is supported by the MS Society of Great Britain and Northern Ireland and the National Institute for Health Research University College London Hospitals Biomedical Research Centre. The MS Society of Great Britain and Northern Ireland has provided financial support for staff and research costs directly associated with this study (grant 917-09).

Tables

Table1 Participant characteristics

	HC	RRMS	SPMS
Number	38	43	28
Mean age, years ± SD (range)	39.1 ± 11.9 (23-63)	42.5 ± 10.0 (25-64)	53.0 ± 8.1 (36-65)
Gender M/F	17/21	14/29	9/19
Median EDSS (range)	NA	2 (1.0-7.0)	6.5 (4.0-8.5)
Disease Duration, years ± SD	NA	11.7 ± 8.1	21.9 ± 10.4
Mean MTR in whole NAWM ± SD	39.7 ± 0.8	38.9 ± 1.5	38.4 ±1.9
Mean number of bands extracted ± SD	44.0 ± 3.2	42.7 ± 3.2	41.1 ± 3.8
Mean BPF ± SD	0.82 ± 0.02	0.80 ± 0.02	0.80 ± 0.03

EDSS = Expanded Disability Status Scale; HC = health controls; NA = not available; NAWM = normal appearing white matter; MTR = magnetisation transfer ratio; RRMS = relapsing-remitting multiple sclerosis; SD = standard deviation; SPMS = secondary progressive multiple sclerosis; BPF = brain parenchymal fraction.

Table 2 Mean MTR values in NAWM bands 1, 5 and 10 from lateral ventricle

Band	Type	Mean (SE) MTR (pu)	Differences
1	HC	41.0 (0.14)	*HC vs RRMS: p<0.001* *HC vs SPMS: p<0.001* *RRMS vs SPMS: p=0. 019*
	All MS	38.9 (0.19)	
	RRMS	39.2 (0.24)	
	SPMS	38.4 (0.27)	
5	HC	40.6 (0.13)	*HC vs RRMS: p<0.001* *HC vs SPMS: p<0.001* *RRMS vs SPMS: p=0.152*
	All MS	39.2 (0.15)	
	RRMS	39.4 (0.20)	
	SPMS	39.0 (0.22)	
10	HC	40.3 (0.14)	*HC vs RRMS: p<0.001* *HC vs SPMS: p<0.001* *RRMS vs SPMS: p=0.258*
	All MS	39.1 (0.14)	
	RRMS	39.3 (0.18)	
	SPMS	39.0 (0.21)	

HC = health controls; MS = multiple sclerosis; MTR = magnetisation transfer ratio; pu = percent units; RRMS = relapsing-remitting multiple sclerosis; SE = standard error; SPMS = secondary progressive multiple sclerosis.

Table 3 MTR gradients between NAWM bands 1, 5 and 10

Bands	Type	Mean (SE) MTR change (pu, per band interval)	Differences
1 to 5	HC	-0.11 (0.01)	*HC vs RRMS: p<0.001* *HC vs SPMS: p<0.001* *RRMS vs SPMS: p=0.027*
	All MS	0.08 (0.03)	
	RRMS	0.04 (0.03)	
	SPMS	0.14 (0.04)	
5 to 10	HC	-0.07 (0.01)	*HC vs RRMS: p=0.007* *HC vs SPMS: p=0.001* *RRMS vs SPMS: p=0.253*
	All MS	-0.02 (0.01)	
	RRMS	-0.03 (0.01)	
	SPMS	-0.01 (0.02)	

HC = health controls; MTR = magnetisation transfer ratio; pu = percent units; RRMS = relapsing-remitting multiple sclerosis; SE = standard error; SPMS = secondary progressive multiple sclerosis.

Figures

Figure 1. NAWM above the superior limit of the insula was segmented into concentric periventricular 1 voxel thick bands.

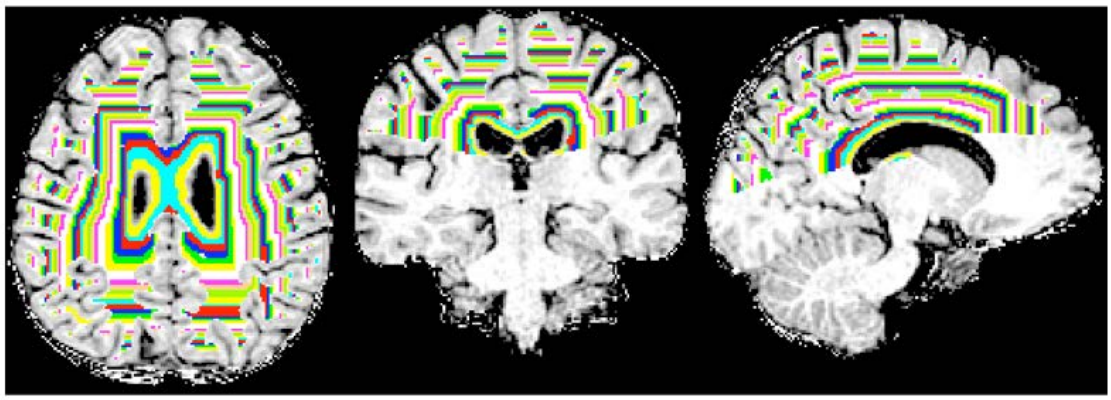

Figure 2. NAWM band MTR in each subgroup, mean ± 2 x standard error. MTR is given in percent units (pu).

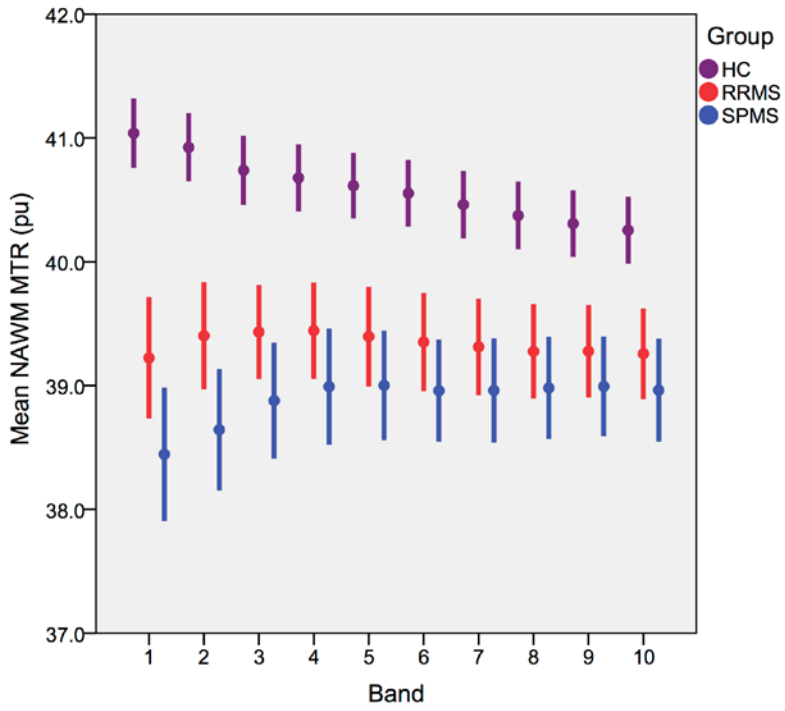

Figure 3a. WM lesion ~~band~~ MTR for each band in the RRMS and SPMS groups, mean ± 2 x standard error.

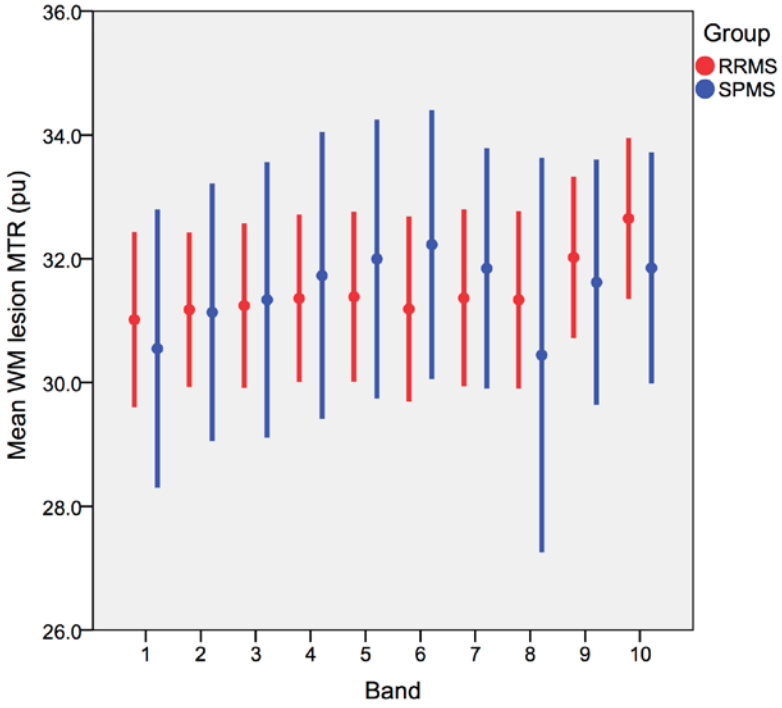

Figure 3b. WM lesion ~~band~~ volume for each band in the RRMS and SPMS groups, mean ± 2 x standard error.

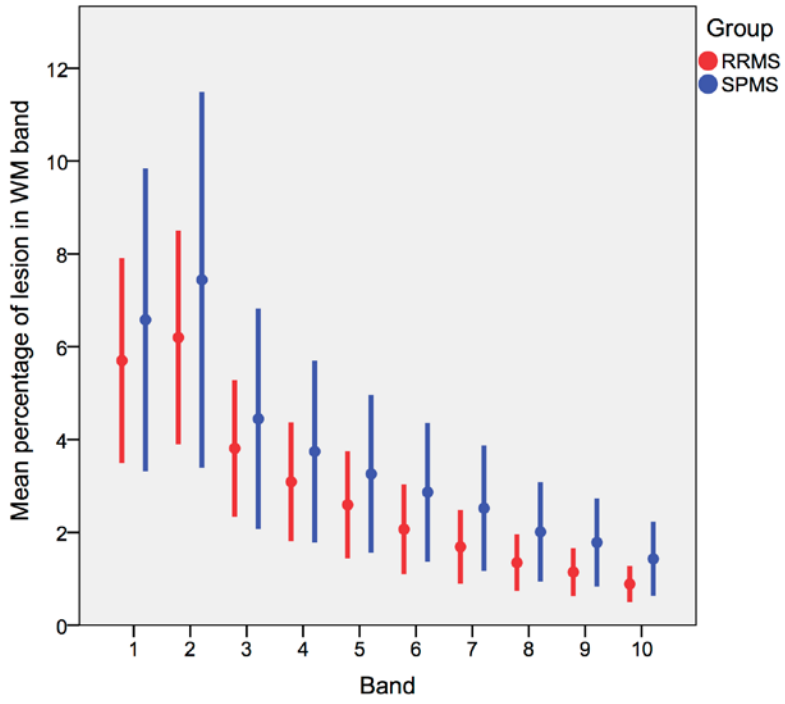

References

Adams CW. The onset and progression of the lesion in multiple sclerosis. J Neurol Sci 1975; 25: 165-82.

Adams CW, Abdulla YH, Torres EM, Poston RN. Periventricular lesions in multiple sclerosis: their perivenous origin and relationship to granular ependymitis. Neuropathol Appl Neurobiol 1987; 13: 141-52.

Adhya S, Johnson G, Herbert J, Jaggi H, Babb JS, Grossman RI, Inglese M. Pattern of hemodynamic impairment in multiple sclerosis: dynamic susceptibility contrast perfusion MR imaging at 3.0 T. Neuroimage 2006; 33: 1029-35.

Beggs, CB. Venous hemodynamics in neurological disorders: an analytical review with hydrodynamic analysis. BMC Med 2013; 11: 142. doi: 10.1186/1741-7015-11-142.

Bo L, Geurts JJ, Mork SJ, van der Valk P. Grey matter pathology in multiple sclerosis. Acta Neurol Scand 2006; 183: 48-50.

Chard DT, Jackson JS, Miller DH, Wheeler-Kingshott, CAM. Reducing the impact of white matter lesions on automated measures of brain gray and white matter volumes. J Magn Reson Imaging 2010; 32: 223-8.

Hickman SJ, Barker GJ, Molyneux PD, Miller DH. Technical note: the comparison of hypointense lesions from ‘pseudo-T1’ and T1-weighted images in secondary progressive multiple sclerosis. Mult Scler 2002; 8: 433–435.

Horsfield, MA. Magnetization transfer imaging in multiple sclerosis. J Neuroimaging 2005; 15: 58S-67S.

Hughes D, Field EJ. Myelotoxicity of serum and spinal fluid in multiple sclerosis: a critical assessment. Clin Exp Immunol 1967; 2: 295-309.

Kearney H, Yiannakas MC, Samson RS, Wheeler-Kingshott CA, Ciccarelli O, Miller DH. Investigation of magnetization transfer ratio-derived pial and subpial abnormalities in the multiple sclerosis spinal cord. Brain 2014; 137: 2456-68.

Kurtzke JF. Rating neurologic impairment in multiple sclerosis: an expanded disability status scale (EDSS). Neurology 1983; 33: 1444-52.

Lassmann H. Hypoxia-like tissue injury as a component of multiple sclerosis lesions. J Neurol Sci 2003; 206: 187-91.

Lassmann H. Multiple sclerosis: Lessons from molecular neuropathology Exp Neurol 2013; http://dx.doi.org/ 10.1016/j.expneurol.2013.12.003

Lublin FD, Reingold SC. Defining the clinical course of multiple sclerosis: results of an international survey. National Multiple Sclerosis Society (USA) Advisory Committee on Clinical Trials of New Agents in Multiple Sclerosis. Neurology 1996; 46: 907-11.

Magliozzi R, Howell O, Vora A, Serafini B, Nicholas R, Puopolo M, et al. Meningeal B-cell follicles in secondary progressive multiple sclerosis associate with early onset of disease and severe cortical pathology. Brain 2007; 130: 1089-104.

Magliozzi R, Howell OW, Reeves C, Roncaroli F, Nicholas R, Serafini B, et al. A Gradient of neuronal loss and meningeal inflammation in multiple sclerosis. Ann Neurol 2010; 68: 477-93.

Maldjian, JA, Laurienti, PJ, Burdette, JB, Kraft RA. An automated method for neuroanatomic and cytoarchitectonic atlas-based interrogation of fMRI data sets. Neuroimage 2003; 19: 1233-9.

Modat M, Ridgway GR, Taylor ZA, Lehmann M, Bames J, Hawkes DJ, et al. Fast free-form deformation using graphics processing units. Comput Methods Programs Biomed 2010; 98: 278-84.

Muhlert N, Sethi V, Schneider T, Daga P, Cipolotti L, Haroon HA, et al. Diffusion MRI-based cortical complexity alterations associated with executive function in multiple sclerosis. J Magn Reson Imaging 2013; 38: 54-63.

Nait-Oumesmar B, Picard-Riera N, Kerninon C, Decker L, Seilhean D, Hoglinger GU, et al. Activation of the subventricular zone in multiple sclerosis: Evidence for early glial progenitors. Proc Natl Acad Sci 2007; l 04: 4694-9.

Narayanan S, Fu L, Pioro E, De Stefano N, Collins DL, Francis GS. Imaging of axonal damage in multiple sclerosis: spatial distribution of magnetic resonance imaging lesions. Ann Neurol 1997; 41: 385-91.

Ourselin S, Roche A, Subsol G, Pennec X, Ayache N. Reconstructing a 3D structure from serial histological sections. Image and Vision Computing 2001; 19: 25-31.

Papadopoulou A, Menegola M, Kuhle J, Ramagopalan SV, D'Souza M, Sprenger T et al. Lesion-to-ventricle distance and other risk factors for the persistence of newly formed black holes in relapsing-remitting multiple sclerosis. Mult Scler 2014; 20: 322-30.

Polman CH, Wolinsky JS, Reingold SC. Multiple sclerosis diagnostic criteria: three years later. Mult Scler 2005; 11: 5-12.

Saindane AM, Law M, Ge Y, G. Johnson JS, Babb, and Grossman RI. Correlation of diffusion tensor and dynamic perfusion MR imaging metrics in normal-appearing corpus callosum: support for primary hypoperfusion in multiple sclerosis. AJNR Am J Neuroradiol 2007; 28: 767-72.

Samson RS, Cardoso MJ, Muhlert N, Sethi V, Wheeler-Kingshott CA, Ron M, et al. Investigation of outer cortical magnetisation transfer ratio abnormalities in multiple sclerosis clinical subgroups. Mult Scler 2014; 20: 1322-30.

Schmierer K, Scaravilli F, Altmann DR, Barker GJ, Miller DH. Magnetization transfer ratio and myelin in postmortem multiple sclerosis brain. Ann Neurol 2004; 56: 407-15.

Vidaurre OG, Haines JD, Katz Sand I, Adula KP, Huynh JL, McGraw CA, et al. Cerebrospinal fluid ceramides from patients with multiple sclerosis impair neuronal bioenergetics. Brain 2014; 137: 2271-86.

Vrenken H, Geurts JJ, Knol DL, Polman CH, Castelijns JA, Pouwels PJ, et al. Normal-appearing white matter changes vary with distance to lesions in multiple sclerosis. AJNR Am J Neuroradiol. 27, 2005-11.

Wegner C, Esiri MM, Chance SA, Palace J, Matthews PM. Neocortical neuronal, synaptic, and glial loss in multiple sclerosis. Neurology 2006; 67: 960–7.